Polym. Bull. (2011) 67:1741–1750
DOI 10.1007/s00289-011-0481-4

ORIGINAL PAPER

Thermal and neutron shielding properties of $^{10}B_2O_3$/polyimide hybrid materials

Yusuf Mülazim · Canan Kızılkaya · Memet Vezir Kahraman

Received: 19 October 2010 / Revised: 17 February 2011 / Accepted: 29 March 2011 /
Published online: 3 April 2011

Abstract In this study, $^{10}B_2O_3$/polyimide (PI) hybrid materials were synthesized with the aim to improve their thermal stability and neutron shielding properties. 3,3′-Diaminodiphenyl sulfone (DADPS) reacted with 3,3′,4,4′-benzophenonetetracarboxylic dianhydride (BTDA) in *N*-methyl-2-pyrrolidone (NMP) and mixed with amine functionalized $^{10}B_2O_3$ to prepare a series of poly (amic acid), meanwhile, corresponding PIs were obtained via the thermal imidization procedures. The morphologies and structures of the prepared hybrid materials were characterized by scanning electron microscopy (SEM) and Fourier transform infrared spectroscopy (FT-IR). The thermooxidative and flame retardancy properties of the PI films were examined by thermogravimetric analysis (TGA) and limiting oxygen ındex (LOI). The experimental results showed that as the amount of functionalized $^{10}B_2O_3$ was increased, flame retardant properties of the hybrid films were increased. Hybrid materials were also irradiated with thermal neutrons. The neutron shielding properties increasing depends on the amount and the distribution of the ^{10}B isotope.

Keywords $^{10}B_2O_3$ · Flame retardancy · Hybrid materials · Polyimide · Neutron shielding

Introduction

Engineering plastics are high-performance polymers used in critical applications because of their outstanding balance of properties. Rigid-rod aromatic PIs are well known as high performance polymers because of their excellent thermal and thermooxidative stability, perfect resistance to solvents, chemicals, radiations, and

Y. Mülazim · C. Kızılkaya · M. V. Kahraman (✉)
Department of Chemistry, Marmara University, 34722 Istanbul, Turkey
e-mail: mvezir@marmara.edu.tr

good mechanical, adhesive, and electrical insulation properties. Due to the excellent combination of such properties, they are widely used in different areas such as heat resistance composites, gas seperation membranes, electronic and aerospace industries, coatings, fibers, automobile, and computers [1–8].

Boric oxide (B_2O_3) is a notable oxide that has been studied over the past 40 years. It is produced commercially by the fusion of boric acid. B_2O_3 has the advantage of high refractive index, extreme hardness, low heat expansion, exhibit nonlinear optical behaviors and also well-known fire retardant in engineering plastics (high impact polystyrene, polyetherketone, etc.). Particularly by adding B_2O_3 to the polymers, the thermal stability can be improved. It has been exploited in many fields like enamels, alloys, fluxes, glass ceramic compositions, and catalyst in organic reactions [9–13].

Neutron capture is the process wherein an atomic nucleus will absorb a neutron. The nuclear industry enriches natural boron to nearly pure ^{10}B. It has a large neutron absorption cross section and is used as a neutron absorber. An enriched ^{10}B compounds have been used for shielding detectors, transportation baskets, disposal equipments, space probes, military applications, boron neutron capture therapy (BNCT), and radioactive wastes. The nuclear reaction of the neutron absorption is $^{10}B(n,\alpha\gamma)\ ^{7}Li$ [14–18].

Hybrid materials are defined as synthetic materials with organic and inorganic components. Development of novel polymeric materials in the future points toward hybrid systems. Organic–inorganic hybrid materials stem from the ability to control the nano-architecture of materials at a very early stage of preparation. Many of the properties and applications of hybrids are dependent on the properties of the precursors. These materials have been used in various fields such as coatings, membranes, optical data transmission and storage, transportation industry, medical materials, supercapacitors, and fire retardant materials [19–23].

In this view, a series of $^{10}B_2O_3$/PI hybrid materials were synthesized from a polyamic acid (PI precursor) and $^{10}B_2O_3$ that is modified with aminoalkoxysilane. The silane coupling agent is used for the modification of boron oxide particle surface. Hybrids were characterized by various tecniques such as contact angle, neutron absorption, stres-strain tests, and SEM. The thermal behavior of hybrid materials was also investigated.

Experimental

Materials

3,3′,4,4′-Benzophenonetetracarboxylic dianhydride (BTDA), 3,3′-diaminodiphenyl sulfone (DADPS), *N*-methyl-2-pyrrolidone (NMP), and boric acid pure ^{10}B isotopes ($H_3^{10}BO_3$) were obtained from Merck. A silane coupling agent 3-aminopropyl-trimethoxysilane was purchased from Dow Corning. Glass panels (50 mm × 100 mm × 3 mm) were used as a substrate in order to prepare free thin films.

Measurements

SEM imaging of the hybrid free films was performed on Philips XL30 ESEM-FEG/EDAX. The specimens were prepared for SEM by freeze-fracturing in liquid nitrogen and applying a gold coating of approximately 300 Å.

FT-IR spectrum was recorded on Perkin Elmer Spectrum 100 ATR-FTIR spectrophotometer. Thermo gravimetric analyses (TGA) of the hybrid free films were performed using a Perkin-Elmer Thermo gravimetric analyzer Pyris 1 TGA model. Samples were run from 30 to 750 °C with heating rate of 10 °C/min under air atmosphere.

The LOI values of the hybrid free films were measured using a FTT (Fire Testing Technology) type instrument, on the test specimen bar of $120 \times 60 \times 3$ mm^3 according to ASTM D2863-08.

Mechanical properties of the hybrid free films were determined by standard tensile stress–strain tests to measure modules, ultimate tensile strength, and elongation at break. Standard tensile stress–strain experiments were performed at room temperature on a Material Testing Machine Z010/TN2S, using a crosshead speed of 5 mm/min.

Contact angle measurements were carried out with a Kruss (Easy Drop DSA-2) tensiometer, equipped with a camera. Analyses were made at room temperature by means of the sessile drop technique. For each sample, at least four measurements were made, and the average was taken. The measuring liquid was distilled water.

Synthesis

Conversion of $H_3^{10}BO_3$ into $^{10}B_2O_3$

Boric acid or orthoboric acid is a white triclinic crystal that is soluble in water. Upon heating in air to above 75 °C, it loses part of its water of hydration to form metaboric acid (HBO_2) at around 130 °C. The metaboric acid can be further dehydrated to boric oxide at around 250 °C [24].

$$H_3^{10}BO_3 \leftrightarrow H^{10}BO_2 + H_2O \tag{1}$$

$$H^{10}BO_2 + H^{10}BO_2 \leftrightarrow H^{10}BO_2{-}H^{10}BO_2 \text{ complex} \tag{2}$$

$$H^{10}BO_2{-}H^{10}BO_2 \leftrightarrow {}^{10}B_2O_3 + H_2O \tag{3}$$

Boric oxide ($^{10}B_2O_3$) functionalization

Functionalization of boric oxide is often used to improve adhesion between the boric oxide and the polymer matrix. Trifunctional alkoxysilanes are widely available and can react with surface hydroxyl groups on inorganic fillers. 3-Aminopropyltrimethoxysilane dispersed in toluene for 20 min at 80 °C. The $^{10}B_2O_3$ was added to the solution and allowed to mix for 1 h. Then the product was filtered, washed with alcohol, and dried in an oven for 12 h at 110 °C.

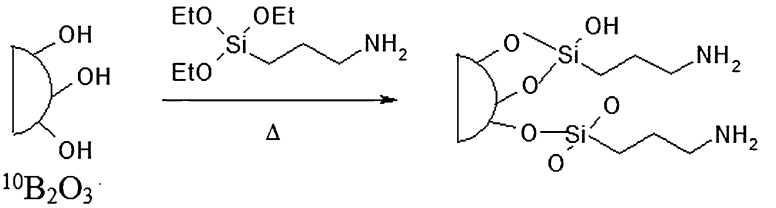

(4)

Preparation $^{10}B_2O_3$/PI of hybrid films

PAA used as a PI precursor was prepared in NMP. DADPS (0.01 mol, 2.485 g) was dissolved in 27.7 ml of dried NMP. Then, BTDA (0.01 mol, 3.22 g) was added in small portions into the above solution. The resulting solution was stirred for 24 h at room temperature under N_2 atmosphere. The solid content of PAA solution was kept at about 20% (w/v). Various amount (0, 0.5, 1, 2, and 5 wt%) of functionalized $^{10}B_2O_3$ was added into the PAA solution with vigorous stirring to minimize the occurrence of local precipitation. After stirring for 1 h, the reaction went to completion. After mixing through stirring, the obtained white color hybrid solution was cast onto the glass plates with the aid of a 30-μm applicator. Then the wet coating was cured at 80, 100, 150, 200, and 250 °C for 1 h at each temperature. The cured hybrid films were retrieved from the glass surface by immersing in distilled water at 80 °C.

Results and discussion

In this work, a series of $^{10}B_2O_3$/PI hybrid materials were synthesized by thermal imidization route, and their mechanical, thermal, and neutron absorption properties were investigated. Totally, five samples with each having different amounts of $^{10}B_2O_3$ content, in the range of 0–5 wt% were prepared. The appearance of the hybrid films was transparent and yellow in color.

The FT-IR spectra of $H_3^{10}BO_3$, $^{10}B_2O_3$, and functionalized $^{10}B_2O_3$ were shown in Fig. 1a. Boric acid has a broad asymmetric B–O stretching band at 1396–1478 cm^{-1}. However, in the actual spectra, there are additional broad peaks that rise from the in plane B–OH bending at 1195 cm^{-1} and out of plane bending at 600–800 cm^{-1}. Additionally, a boric acid peak at 570 cm^{-1} can be attributed to O–B–O bending. It is already known that the broad band at around 3200 cm^{-1} (similar to the mentioned 1195 cm^{-1} peak) is related to O–H stretching bonds. After the thermal treatment, $H_3^{10}BO_3$ is converted to $^{10}B_2O_3$. This is confirmed by the observation of the characteristic absorption bands of B=O stretching at 1566–1600 $cm^{-1}$and disappearance of the peaks at 3200 and 1195 cm^{-1} which corresponds to O–H and B–OH bands, respectively. These results clearly indicate that most of the boric acid has been converted to the boric anhydride. The FT-IR

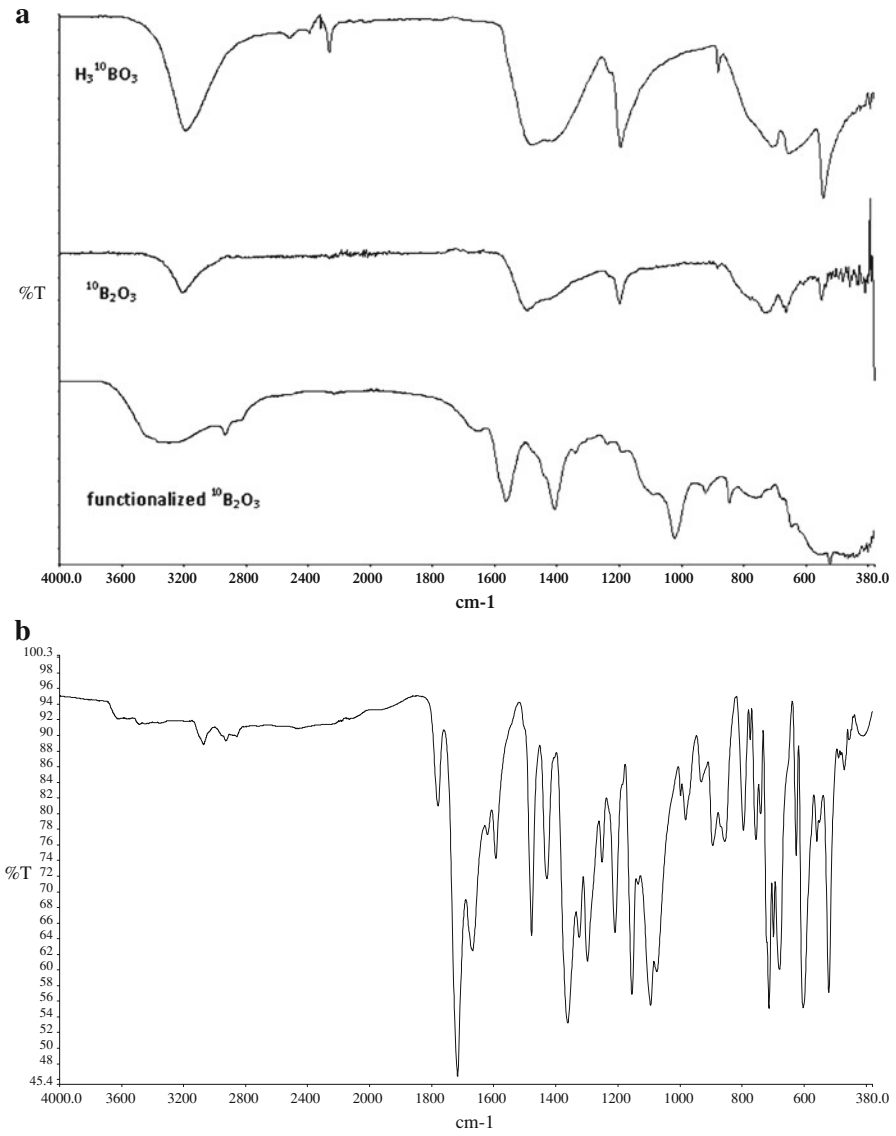

Fig. 1 **a** FT-IR spectra of $H_3^{10}BO_3$, $^{10}B_2O_3$, and functionalized $^{10}B_2O_3$. **b** FT-IR spectra of polyimide (PI-5)

spectra of functionalized $^{10}B_2O_3$ is also shown in Fig. 1a. The absorption bands in the 1000 and 1200 cm^{-1} region indicating the characteristic Si–O–C bonds [25–27].

The spectra for PI-5 PI hybrid film was shown in Fig. 1b. Sample exhibited the characteristic peaks of symmetric and asymmetric C=O stretching of the imide group at 1720 and 1780 cm^{-1}, respectively. Additionally, C–N stretching of the imide ring was observed at 1361 cm^{-1}. The strong absorption bands were observed

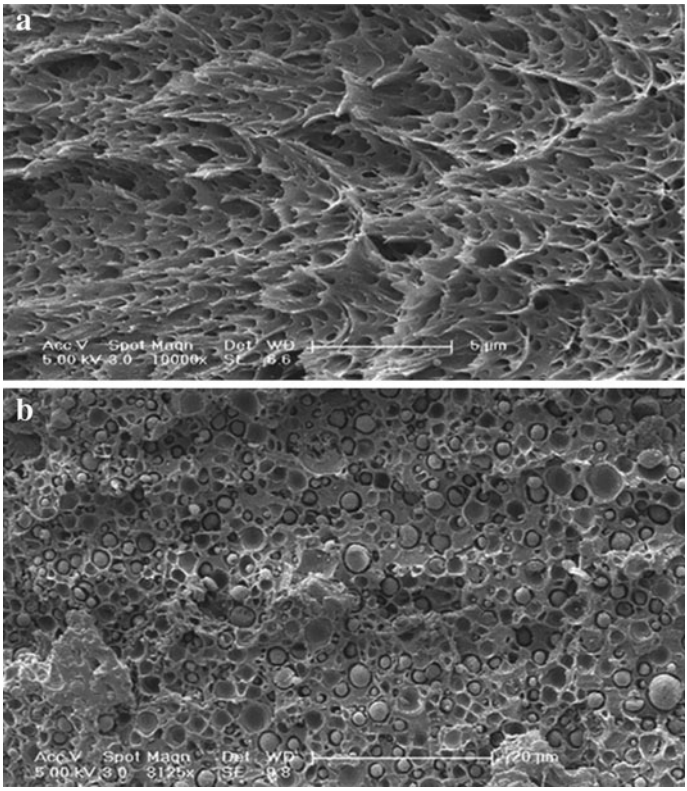

Fig. 2 SEM micrographs of **a** PI and **b** PI-5

at the range of 1000–1100 and 471 cm^{-1}. These bonds were ascribed to the characteristic Si–O–Si stretching vibration and bending vibration, respectively [28, 29].

The SEM micrographs of the fracture surface of the pure PI film and hybrid film ($^{10}B_2O_3$ content 5 wt%) are shown in Fig. 2a and b. As shown in Fig. 2a, the pure PI has porous structure. Additionally, as can be seen from Fig. 2b, the pores are filled by $^{10}B_2O_3$ particles. The $^{10}B_2O_3$ particles are relatively large and debonded from the surrounding PI matrix, indicating relatively poor compatibility between the PI and $^{10}B_2O_3$ phases. The average diameter of $^{10}B_2O_3$ particles varies from 0.5 to 3 μm. The morphology is the result of a typical phase separation by spinodal decomposition differing from each other in the extent of phase connectivity.

Evaluated stress–strain data of hybrid films as tensile modulus, tensile strength, and elongation at break are listed in Table 1. As can be seen in Table 1, the tensile strength, tensile modulus, and elongation at break decreased monotonously with the increasing amount of $^{10}B_2O_3$ content. Lower strength and modulus are expected behaviors if there is weak bonding between the organic polymer phase and the inorganic phase. These results demonstrate that the hybrid films with higher inorganic content behave as hard and brittle.

Table 1 Stress–strain analysis of hybrid films

Sample	Tensile modulus (MPa)	Tensile strength (MPa)	Elongation at break (%)
PI	1764 ± 18	608 ± 8	5.14 ± 0.08
PI-0.5	1706 ± 16	426 ± 6	3.57 ± 0.07
PI-1	1541 ± 11	405 ± 4	3.37 ± 0.07
PI-2	1461 ± 11	347 ± 4	2.96 ± 0.05
PI-5	1302 ± 10	339 ± 3	2.02 ± 0.03

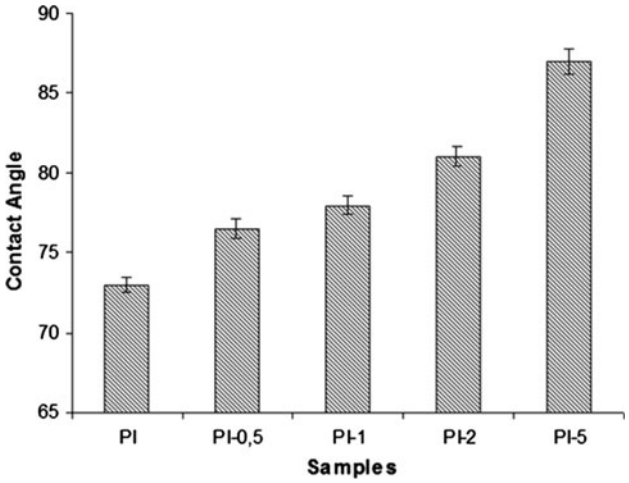

Fig. 3 Contact angle values of hybrids with water

The surface wettability properties of the $^{10}B_2O_3$/PI hybrid materials were investigated by water contact angle measurements. Contact angles are very sensitive to the surface composition changes. Each contact angle value given in (Fig. 3) represents an average of 3–5 readings. As it can be seen in Fig. 3, there is a slight enhancement in contact angle values as the $^{10}B_2O_3$ content of the hybrids increases. The main reason of this increase can be attributed to the apolarity of the boron groups. Apolar character of the pendant $^{10}B_2O_3$ decreases the surface energy and makes the surface more hydrophobic.

We have measured the absorbing power of the proposed hybrid coatings while the thermal neutron lights were applied for 1 min on the coated glass panels. During this measurement, test plates were placed to Howitzer Neutron Source and the number of neutrons, which had passed from the plates, measured by Identifinder Target apparatus. It can be seen from Fig. 4, the ^{10}B-enriched hybrid coatings have high neutron shielding ability. The reasons such as geometry of the detector, distance of the plates to the light source, thickness of the coatings affect the measured neutron shielding capacity.

Figure 5 shows the thermal degradation behaviors of hybrid films and pure PI film. TGA measurements were carried out under air atmosphere at heating rate

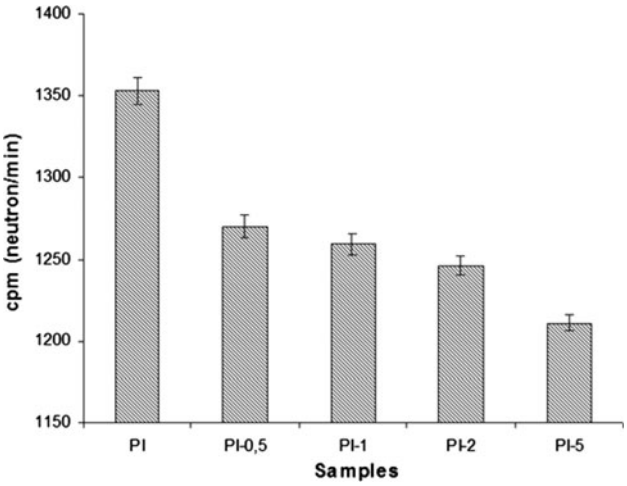

Fig. 4 Neutron absorption capacity of ^{10}B-containing hybrid materials

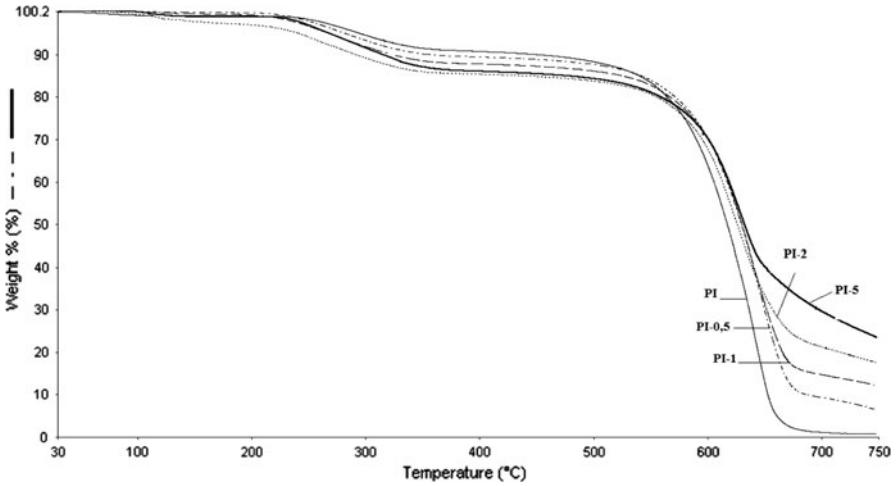

Fig. 5 TGA thermograms of hybrid materials

10 °C/min from room temperature to 750 °C, and the test data are summarized in Table 2. All samples showed 5 wt% weight loss between 271 and 286 °C due to the evaporation of residual solvents such as NMP, ethanol and pure PI can be assigned to incomplete imidization. Decomposition temperatures were realized around 595–609 °C. The flame retardant properties of the boron containing PIs were studied in terms of char yields and LOI values. For these materials, the char yields at 750 °C were 0.8–23.5%. The high char yields of these hybrids at high temperature region are important. It shows that these polymers have excellent thermal stability.

Table 2 TGA analyses of hybrid films

Samples	T_5^a (°C)	T_d^b (°C)	Char yield (%)
PI	286	595	0.8
PI-0.5	282	597	6.6
PI-1	278	605	12.3
PI-2	271	606	17.6
PI-5	273	609	23.5

[a] Measured by TGA at 10 °C/min under air atmosphere and determined at the temperature of 5 wt% weight loss

[b] Decomposition temperature of polyimide films

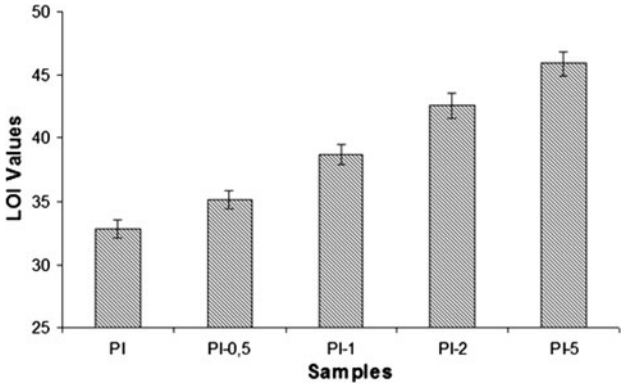

Fig. 6 LOI values of hybrid materials

Figure 6 shows that the LOI values increase from 33 to 46. Consequently, $^{10}B_2O_3$ containing hybrid materials show greater fire resistance than the PI control formulation. The above-mentioned LOI values of the $^{10}B_2O_3$/PI hybrid materials imply that these are effective in flame retardancy. The flame retardancy is related to the formation of a surface layer of protective char, which acts as a barrier to the access of oxygen to prevent the oxidation of carbons.

Conclusion

We report here the synthesis of a series of a novel $^{10}B_2O_3$ containing PI transparent hybrid materials and studied their thermal, mechanical, and neutron shielding properties. FT-IR spectra collected from the boron oxide was correlated very well with the spectral data obtained from a reference boron oxide samples. The results from TGA and LOI showed that as the amount of $^{10}B_2O_3$ was increased, flame retardancy was increased. The neutron absorption test results also clearly indicated that the hybrid materials showed a significant enhancement in radiation shielding properties.

References

1. Chang CC, Chen WC (2002) Chem Mater 14:4242
2. Walsh CJ, Mandal BK (2001) Chem Mater 13:2472
3. Mokhtari I, Bas C, Marestin C, Schiets F, Bartholin M (2008) Eur Polym J 44:832
4. Sun X, Yang YK, Lu F (1998) Macromolecules 31:4291
5. Faghihi K, Shabanian M, Emamdadi N (2010) Macromol Res 18:753
6. Tsai PF, Wu CF, Hsaio CY, Shau MD (2009) J Polym Res 16:673
7. Ahmad Z, Mark JE (2001) Chem Mater 13:3320
8. Hu Z, Wang M, Li S, Liu X, Wu J (2005) Polymer 46:5278
9. Demir H, Şahin O, Izgi MS, Fıratoğlu H (2006) Thermochim Acta 445:1
10. Buc D, Bello I, Caplovicova M, Mikula M, Kovac J, Hotovy I, Chong YM, Siu GG (2007) Thin Solids Films 515:8723
11. Smolanoff J, Lapicki A, Kline N, Anderson SL (1995) J Phys Chem 99:16276
12. Ramos MA, Moreno JA, Vieira S, Prieto C, Fernandez JF (1997) J Non-Cryst Solids 221:170
13. Hu ZB, Li HJ, Fu QG, Xue H, Sun GL (2007) N Carbon Mater 22:131
14. Celli M, Grazzi F, Zoppi M (2006) Nucl Instrum Methods Phys Res A 565:861
15. Sakurai Y, Sasaki A, Kobayaski T (2004) Nucl Instrum Methods Phys Res A 522:455
16. Kharita MH, Takeyeddin M, Alnassar M, Yousef S (2008) Prog Nucl Energy 50:33
17. Smith MHS, Van Buuren LD, Doyle JM, Dzhosyuk SN, Gilliam DM, Mattoni CEH, Mckinsey DN, Yang L, Huffman PR (2004) Nucl Instrum Methods Phys Res B 215:531
18. Paquis P, Pignol JP, Lonjon M, Brassart N, Courdi A, Chauvel P, Grellier P, Chatel M (1999) J Neurooncol 41:21
19. Corriu RJP, Leclercq D (1996) Angew Chem Int Ed Engl 35:1420
20. Rösch J (1995) Polym Eng Sci 35:1917
21. Rösch J, Mülhaupt R (1994) Polym Bull 32:697
22. Pinnavaia TJ, Beall GW (2002) Polym Int 51:464
23. Ashby MF, Brechet YJM (2003) Acta Mater 51:5801
24. Slutskii VG, Severin ES, Polenov LA (2007) Khimicheskaya Fizika 26:22
25. Zha C, Atkins GR, Masters AF (1998) J Non-Cryst Solids 242:63
26. Ivanova Y, Vueva Y, Figueira Vaz Fernandes MH (2006) Chem Mater 41:417
27. Buc D, Bello I, Caplovicova M, Mikula M, Kovac J, Hotovy I, Chong YM, Siu GG (2007) Thin Solid Films 515:8723
28. Tsai MH, Whang WT (2001) Polymer 42:4197
29. Huang Y, Gu Y (2003) J Appl Polym Sci 88:2210